The physics of the low energy tail in the ACIS CCD. The Spectral Redistribution Function.

G. Prigozhin (MIT), S. Jones (MIT),

M. Bautz (MIT), G. Ricker (MIT), S. Kraft (PTB, BESSY)

Abstract

We studied the response of high-resistivity MOS CCDs to monochromatic X-ray illumination at energies ranging from 1.47 to 5.9 keV and discovered a new feature in the low energy tail of the response function. We attribute it to the photons interacting in the gate insulator and explain the shape of the entire low energy tail assuming that it is formed by electron charge clouds partially formed in the gate oxide. The size of the charge clouds derived from this model is much smaller than previously reported. This can be explained by a different field distribution in a buried channel CCD.

1 Introduction

X-ray CCDs have become a popular tool for soft X-ray imaging and spectroscopy, especially in high-energy astrophysics. Calibration of these devices for astronomical purposes requires a precise knowledge of the device spectral redistribution function at any energy within the range of interest (typically, from 200 eV to 15,000 eV).

The response of the frontside-illuminated CCDs to monochromatic X-rays shows a noticeable low energy tail in addition to the well understood main peak and escape and fluorescence features.

It is generally assumed for silicon detectors that the tail's origin is due to dead layer on the surface of the device [1, 2]. We have studied the response of the CCD to monochromatic X-rays in a wide range of energies and have discovered a previously unreported feature in the very low energy part of the response function. Examining changes in its behavior as a function of the energy of the incoming radiation, we came to the conclusion that this feature originates from the photons interacting in the gate insulator, which is therefore not a dead layer as was previously thought. We have developed a model that explains the shape of this newly discovered feature as well as the shape of entire low energy tail in the CCD response function.

2 Experimental

The CCDs used in this study were manufactured at MIT Lincoln Laboratory for the Advanced X-ray Astrophysics Facility (AXAF). They are frame transfer devices comprised of a frame store and an image section 1024 x 1026 pixels each, identical to the devices installed in the focal plane of the AXAF CCD Imaging Spectrometer (ACIS). They are manufactured on a high resistivity $p-$ type substrate (approximately 5000 Ohm·cm) in order to improve X-ray sensitivity.

The gate structure of the device consists of the gate insulator (a sandwich of $SiO_2 - Si_3N_4 - SiO_2$) covered by the phosphorus-doped polysilicon gates. It has a regular three-phase three polysilicon layer architecture. A detailed description of the device can be found in [3].

Experimental data were acquired at the electron storage ring BESSY (Berlin), where the device cooled to -120^o C was illuminated with monochromatic X-rays. The data were taken at the KMC (Krystal MonoChromator) beamline at energies between 1487 eV and 5898 eV with special emphasis on the understanding of the device behavior around silicon absorption K edge (1839 eV). That explains the choice of the energy data points for this measurement having higher density around silicon K edge: 1487, 1700, 1740, 1800, 1825, 1832, 1835, 1836.5, 1838, 1840, 1842, 1845, 1847, 1855, 1870, 1900, 2015, 2309, 2622, 3313, 3691, 4090, 4510, 4952, 5414, and 5898 eV. The typical exposure time at each energy was 4000 seconds, with 5 times that exposure for the 2015 eV measurement.

The device was clocked by computer-controlled electronics with a serial register clock frequency of 100 kHz, total system noise at this frequency being about 2 electrons *rms*. This low system noise was crucial factor that allowed us to observe the low energy features discussed below.

3 Low energy peak

Fig. 1 shows the histogram of the CCD response to a monochromatic beam of 1700 eV X-rays.

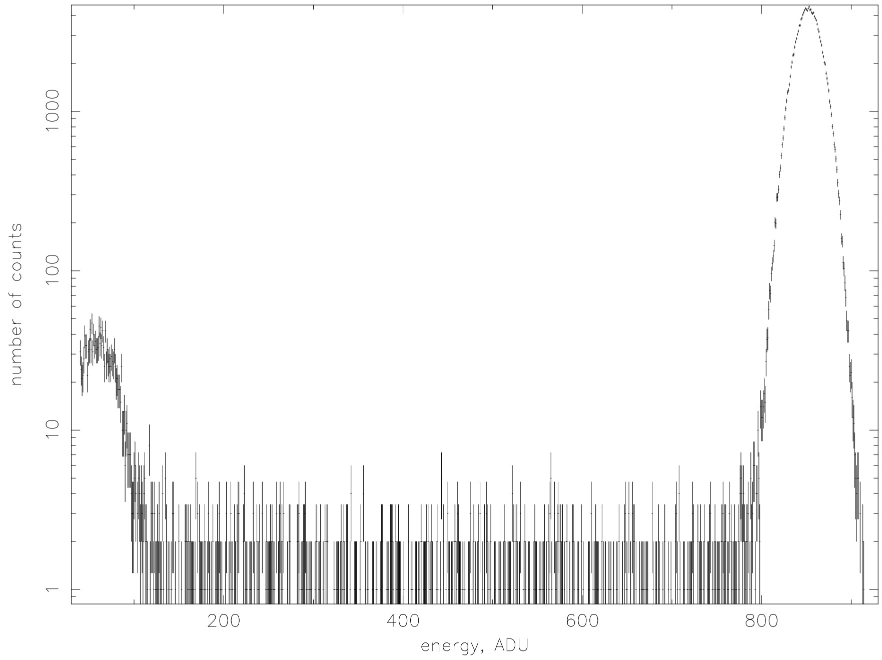

Figure 1: Histogram of the CCD response to 1700 eV X-rays.

This histogram is typical for the device response at energies below the silicon absorption K edge. It has two distinct peaks - the main one, which corresponds to the energy of the incoming photons, and the second one at an energy equal to 7% of the main peak energy. Notice that since 1700 eV is below the silicon K absorption edge energy, silicon fluorescence does not play any role here.

The shape of the low energy peak is not gaussian, though it is possible to make a gaussian fit of reasonable quality. Having done that at different energies we found that the centroid of the low energy peak moves approximately proportionally to the centroid of the main peak (which is known to be a linear function of the energy of irradiating photons), as it is shown in Fig 2. Such behavior

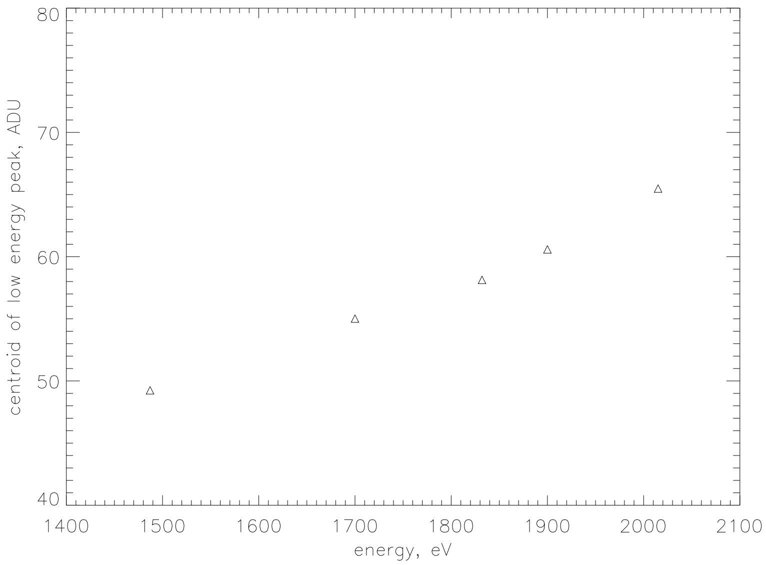

Figure 2: Centroid of the low energy peak as a function of energy.

is different, for instance, from the silicon escape peak for which energy shift is exactly the same as for the main peak.

Another important observation is that total number of counts in the low energy peak is consistent with the number of calculated photon interactions within the gate isolator.

If we assume that the gate insulator consists of a layer of SiO_2 with thickness d_{ox} and characteristic absorption length λ_{ox}, the number of photons per unit area N_{ox} absorbed in it is

$$N_{ox} = N_0(1 - \exp{(-\frac{d_{ox}}{\lambda_{ox}})}) \tag{1}$$

where N_0 is photon flux entering SiO_2 layer. The number of photons N_{si} that are absorbed inside the volume of silicon and form the main peak in the histogram is simply the entire flux of photons entering silicon, since the thickness of the depleted layer of silicon d_d is large compared to the characteristic absorption length in silicon λ_{si} at these energies. Due to attenuation in the gate oxide $N_{si} = N_0 \exp{(-\frac{d_{ox}}{\lambda_{ox}})}$. This gives the ratio of the intensities for the two peaks:

$$\frac{N_{ox}}{N_{si}} = (e^{\frac{d_{ox}}{\lambda_{ox}}} - 1) \tag{2}$$

In the case $d_{ox} \ll \lambda_{ox}$ which is definitely true at energies below the silicon absorption K edge, equation (2) becomes

$$\frac{N_{ox}}{N_{si}} = \frac{d_{ox}}{\lambda_{ox}} \tag{3}$$

Fig. 3 shows the ratio of the number of events in the low energy peak to the number of events in the main peak as a function of energy. The dashed line in this Figure is the result of the

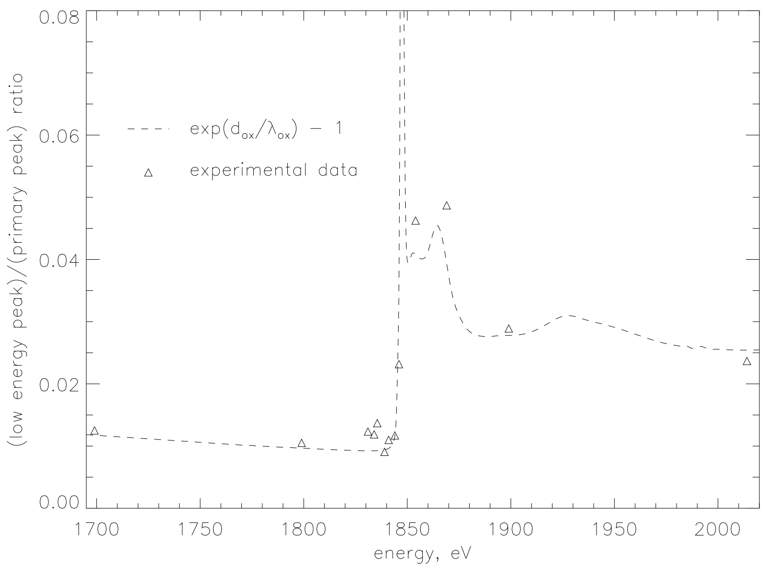

Figure 3: Ratio of number of counts in low energy peak and in the primary peak as a function of energy, calculated (dashed line), and measured (triangles).

calculation according to equation 2. The dependence of λ_{ox} on energy comes from our high precision experimental measurement of the absorption coefficient of the SiO_2 film (see [4]) and includes all the details of the near-edge absorption structure. The relative number of counts in the low energy peak jumps up sharply at the energy corresponding to the silicon K absorption edge, in a good agreement with the prediction of the equation 2.

The most remarkable feature of this plot is that the jump occurs at the energy corresponding to the silicon absorption edge in SiO_2, which is different from the silicon absorption edge in the crystalline silicon. We have shown in [4] that there exists a 6 eV difference between the silicon absorption edge energies in Si and SiO_2. Three data points in Fig 3 lie between the two edges, and are at the same level as the points below the edge in Si, demonstrating conclusively that the low energy peak originates in the SiO_2 layer.

Unlike diode-type detectors or $p-n$ junction CCDs [2], buried channel CCDs have a nonzero electric field in the gate oxide covering silicon surface. This field pulls electrons towards collecting potential wells and this is the reason why the low energy peak we observe in CCD had not been seen in other devices. In Fig. 4 is shown a distribution of the potential in the gate structure of the buried channel CCD.

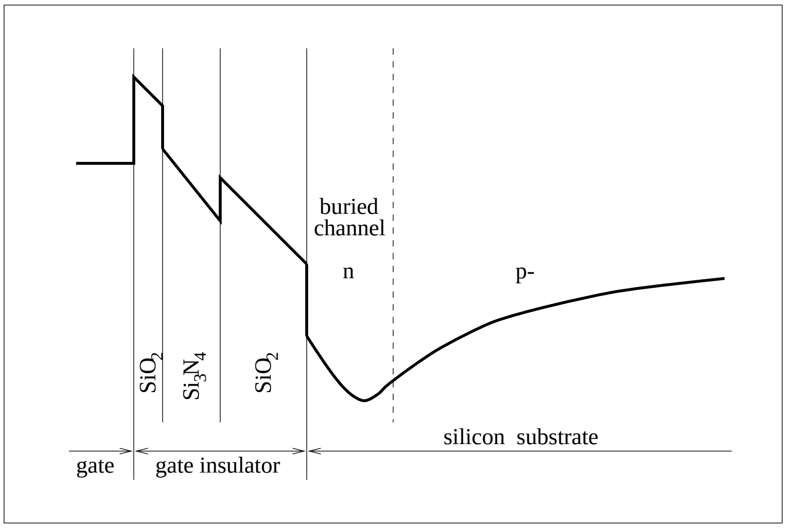

Figure 4: Potential distribution in the buried channel CCD.

When an X-ray photon interacts in the gate oxide layer, it generates a cloud of electron-hole pairs. The energy required to create one electron-hole pair in SiO_2 is reported to be 17 eV [5]. Under the influence of the electric field electrons are swept out of oxide layer into the silicon ending up in the potential wells of the CCD, while holes move very slowly towards the polysilicon gate. Although electrons leave the oxide layer in a very short period of time (with the mobility of 40

$cm^2/(V \cdot s)$ at low temperatures [6], the drift time through the gate oxide is on the order of a picosecond), a significant number of them is lost due to recombination in the SiO_2 layer. According to [7] the fraction of surviving electrons can vary widely depending on the electric field and the photon energy. As a result the corresponding peak in the histogram is seen at very low energy. Assuming electron-hole pair creation energy in SiO_2 is 17 eV, our results indicate that 65% of electrons created there are lost.

So far we have discussed only data taken at energies around silicon K edge. The picture is very different at higher energies. At 5414 eV (a histogram of the device response is shown in Fig. 5) instead of the well-defined low energy peak shifted further up from what we see at 1700 eV histogram, there is a broad elevation which goes all the way down to the noise peak (not shown) without reaching a maximum. We believe that the reason for such behavior is an increased electron

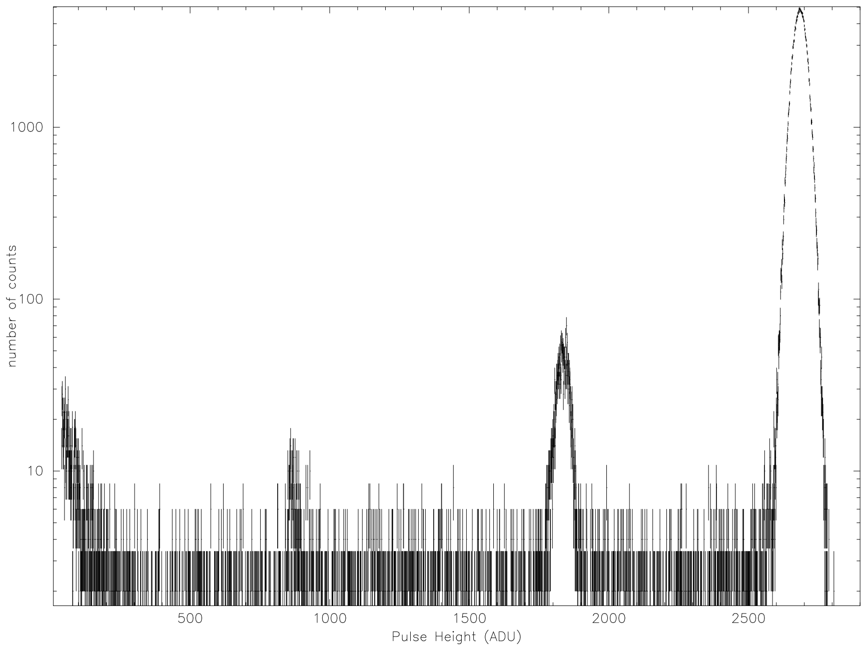

Figure 5: Histogram of the CCD response to 5414 eV X-rays.

cloud size at higher energies. It is known that the diameter of the electron cloud generated by a photon increases with energy and according to various authors could be tens or even hundreds of nanometers at several keV [1, 2, 8]. The gate oxide layer is very thin, approximately 70 nm and its thickness is comparable to the cloud size. When the cloud diameter exceeds the oxide thickness, any cloud originated in silicon dioxide deposits some charge either in silicon, or in silicon nitride. The amount of charge escaping the oxide depends on the photon's depth of interaction. There exists a potential barrier for the electrons that are moving from Si_3N_4 into SiO_2 (see Fig. 4), which means that part of the cloud that enters Si_3N_4 will be almost entirely lost. For the events that originate in Si_3N_4 only electrons with sufficiently high energy can overcome the potential barrier.

Thus, even small changes in the depth of interaction of the original photon in the SiO_2 layer lead to significant changes in the total number of electrons collected, and as a result the low energy peak is washed out into a much broader feature without an extremum.

4 The shape of the low energy tail

A similar phenomenon - splitting of the cloud between silicon and silicon dioxide - should obviously take place for any cloud which originates within the distance R from the $Si - SiO_2$ interface, where R is the cloud radius. Since the number of the electron-hole pairs generated per eV of the incoming photon energy in silicon is significantly higher in silicon than in silicon dioxide, the amplitude of such events will change gradually from the primary peak down to the low energy peak, as the center of the cloud moves from silicon into oxide. This is schematically shown in Fig. 6, which explains how the low energy tail of the spectral redistribution function is formed. Fig. 7 provides evidence that the entire low energy tail comes from the photons interacting within a small distance from the silicon interface. This figure shows the fraction of events in the tail as a function of the characteristic absorption length λ_{si} in silicon. In order to produce this plot events in the fluorescent and in the escape peaks were ignored, as well as the low energy (oxide) peak events discussed in section 3. Each point in this plot corresponds to a measurement at a particular energy, and the points are connected sequentially in energy ascending order, starting at the lowest energy point

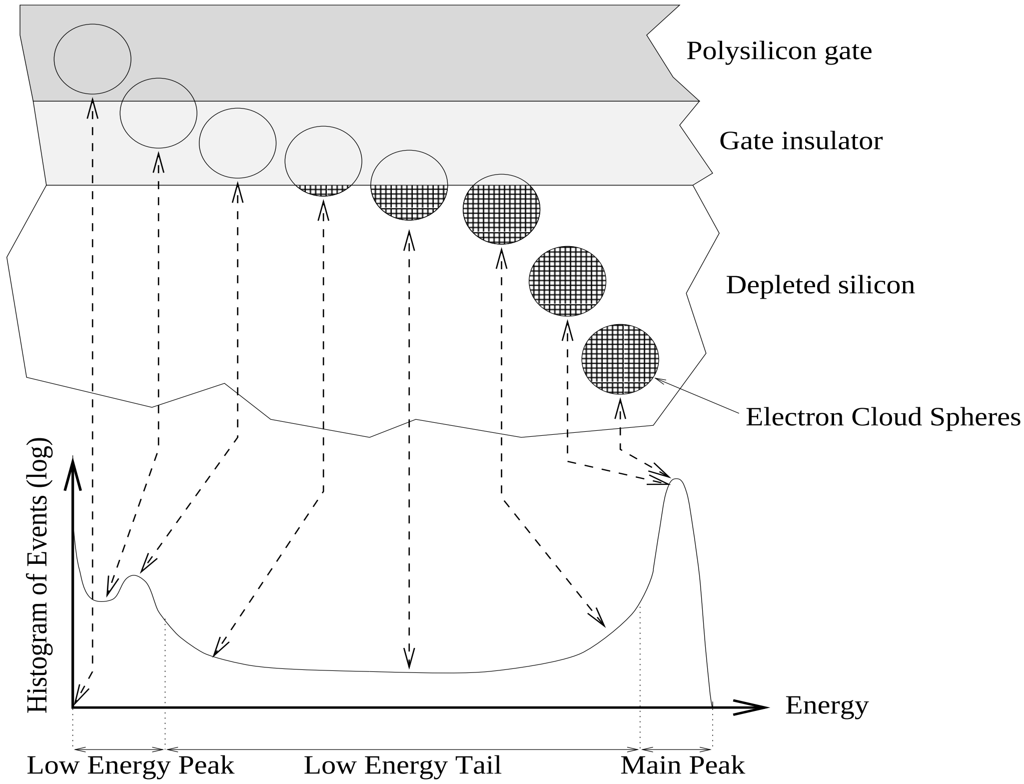

Figure 6: Scheme of forming low energy tail from the electron clouds generated close to $Si - SiO_2$ interface.

labeled 1487 eV. The plot demonstrates that for widely separated energies (for instance, 1487, 1836, and 3600 eV) with the similar values of λ_{si}, the fraction of events in the tail is similar. Moreover, immediately above the silicon, edge at very small λ_{si}, the tail intensity goes up sharply. If one makes a very crude assumption that the cloud radius R is constant (or slowly changing function of energy in the range of interest), then an approximately $1/\lambda_{si}$ dependence is an indication that the flat part of the tail results from the the photons interacting in a shallow region near the surface, whose thickness $2R$ is small compared to λ_{si}.

If all the events in the flat part of the low energy tail come from the electron clouds formed within a distance R of the $Si - SiO_2$ interface, the fraction of the events in the flat part of the tail can be used to determine the electron cloud size. The results of such calculations are shown in Fig. 8, and are discussed in more detail in the following section. The precise shape of the tail

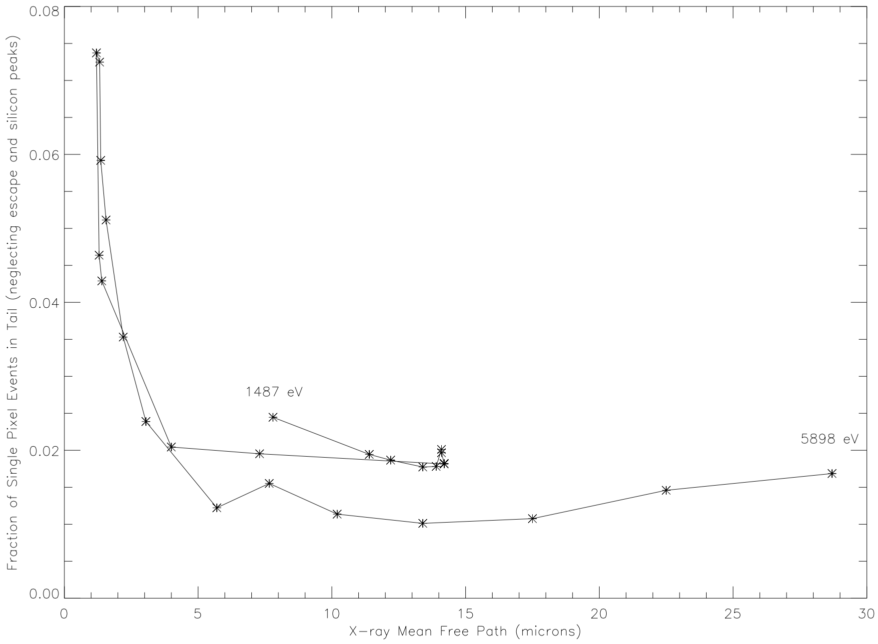

Figure 7: Fraction of single pixel events in tail as a function of characteristic absorption length in silicon.

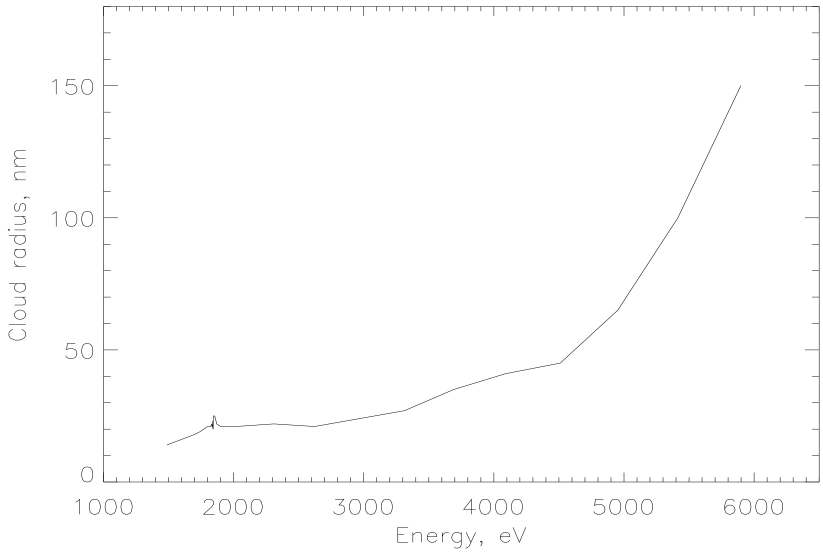

Figure 8: Cloud radius in silicon as a function of energy.

depends on the density distribution of charge in the cloud and this distribution in principle can be extracted. We have not accomplished this task however, because it requires a larger quantity of data than we were able to obtain during the limited time at the synchrotron facility.

5 A model of the low energy tail

We have developed a model based on the scheme shown at Fig. 6. The basic assumption is that each electron cloud is a sphere and when the sphere crosses the silicon interface, the number of electrons produced in each material is proportional to the volume of the corresponding segment of the sphere. Each material is assumed to have different electron-hole creation energy. This is equivalent to assuming that electrons have the same mean free path in both materials. This may be not such a bad approximation, especially for high energy electrons in the original stages of cascading. As discussed above, electrons liberated in the oxide contribute to the total charge collected. From the low energy peak position (see Fig. 2) we deduce an effective electron-hole pair creation energy w_{ox} in SiO_2 of approximately 52 eV. This value includes recombination losses and hence differs significantly from the value reported in [5]. We have made no attempt here to decouple the true value of w_{ox} and the losses. This matter is clearly worth pursuing, because a CCD offers a unique opportunity to measure directly the charge generated in the oxide layer.

Figures 9 - 12 compare the best fit of the model to the data at several energies.

One of the free parameters adjusted to fit the model to the data is the cloud radius R. The energy dependence of the best-fit R is shown in Fig. 8. The values of cloud sizes are significantly lower than $150 - 200$ nm reported in [1, 2]. We believe the reason for this large discrepancy is the presence of a high potential barrier for electrons (approximately 3.5 eV) at the $Si - SiO_2$ interface. Electron cloud generation starts with emission of relatively high energy primary photo- and Auger electrons which dissipate their energy in an ionization cascade. The range of electrons in the initial stages of the cascade is roughly consistent with the cloud radius in our model. It is the low energy, nearly thermalized electrons with sharply increased mean free path (of an order of 100 nm) that are responsible for the large cloud sizes quoted in [1, 2]. In the MOS structure analyzed here a "potential wall" at the $Si - SiO_2$ interface prevents the low energy electrons from penetrating

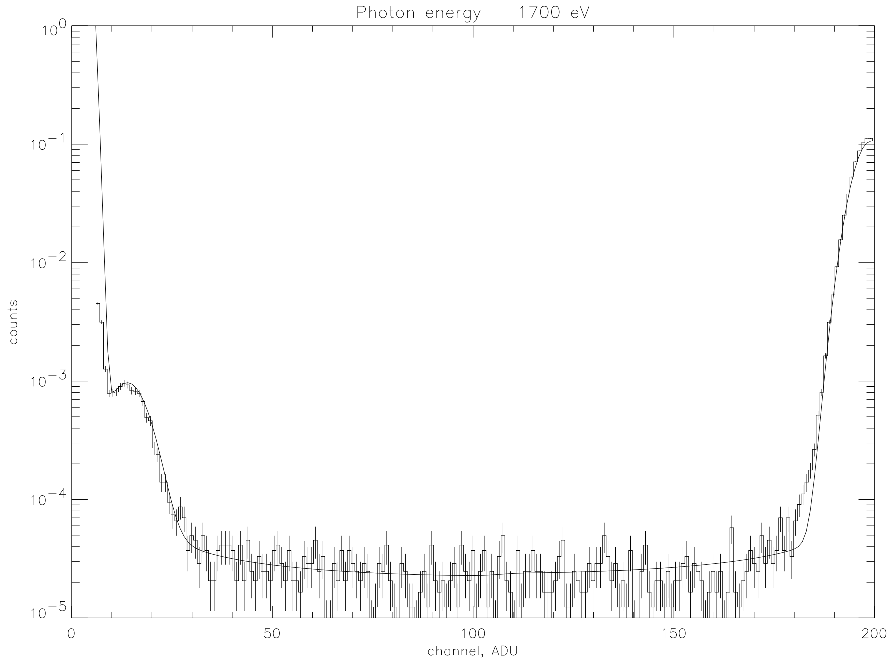

Figure 9: Response of the CCD to the 1700 eV photons and the model prediction.

into the SiO_2 for the clouds centered at a distance greater than R from this interface. Only hot electrons in the initial stages of cascading (for which the range is very small) can participate in the cloud splitting between the silicon and the silicon dioxide. This feature of MOS X-ray CCDs is

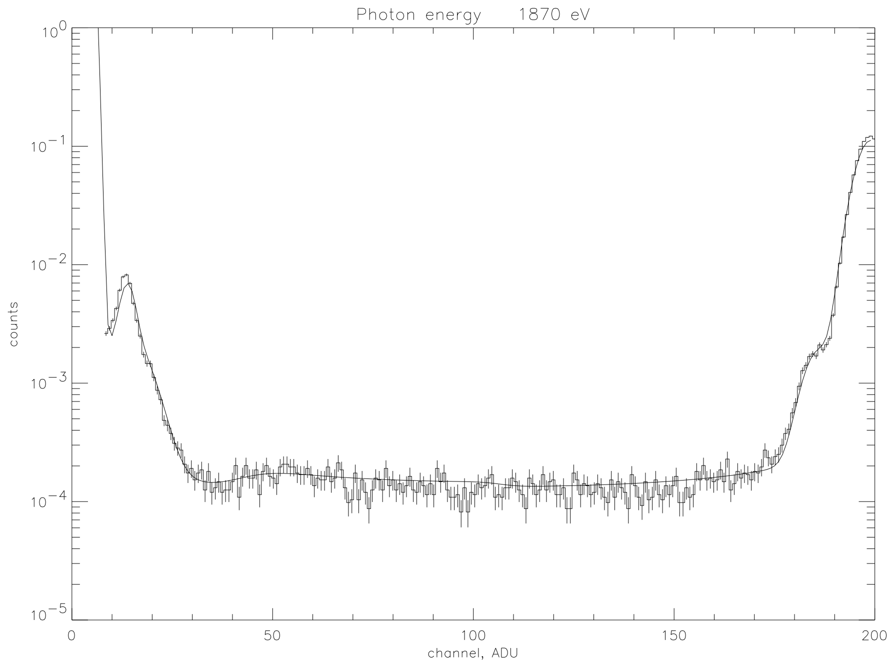

Figure 10: Response of the CCD to the 1870 eV photons and the model prediction.

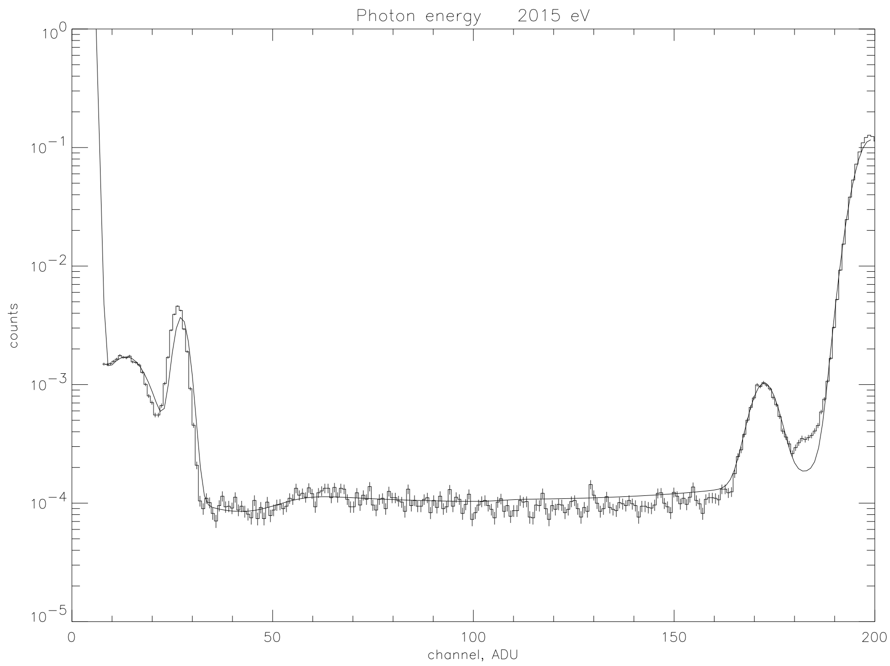

Figure 11: Response of the CCD to the 2015 eV photons and the model prediction.

very beneficial for the spectrometric properties of the frontside illuminated devices, since it results in larger fraction of counts going into the main peak instead of the tail, and, hence, better energy resolution and quantum efficiency.

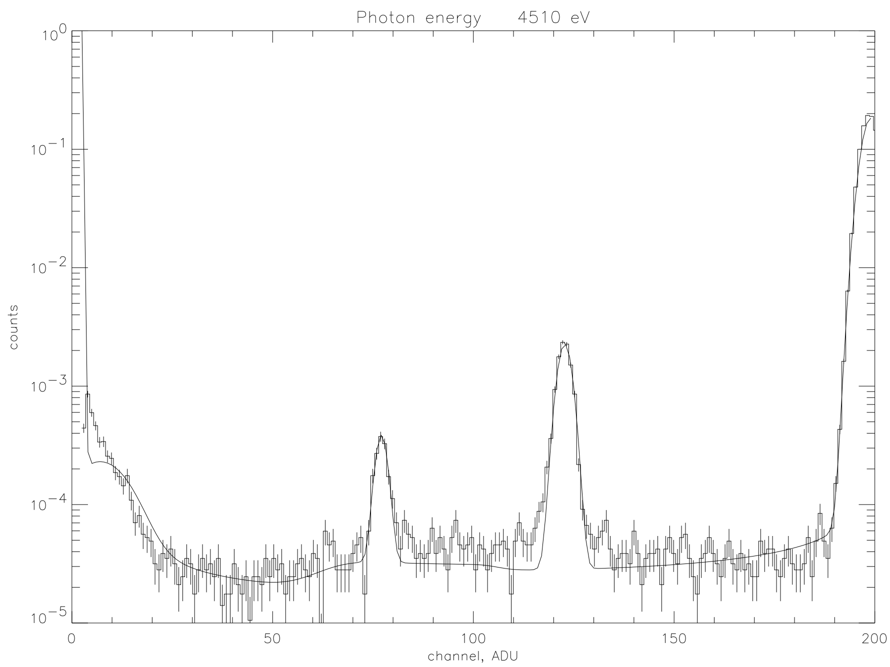

Figure 12: Response of the CCD to the 4510 eV photons and the model prediction.

6 Conclusion

We have discovered a previously unreported feature in the low energy part of the response function of the MOS X-ray CCD. This feature is produced by the electrons generated in the SiO_2 layer which covers the surface of silicon and is reasonably well described by a model that accounts for splitting of the charge cloud between two layers with different energies of electron-hole pair creation. The same model explains the shape of the entire low energy tail over a wide range of energies. An important finding is that charge from the silicon dioxide layer can be collected and so is not necessarily lost. The charge cloud radius near the $Si - SiO_2$ interface is much smaller than in the silicon bulk due to reflection of low energy nearly thermalized electrons from the potential barrier at the interface.

7 Acknowledgment

The authors gratefully acknowledge the effort of people who helped us during the data acquisition at BESSY: Steve Kissel, Michael Pivovaroff, Frank Scholze. This work was funded by NASA as a part of the ACIS calibration program.

References

[1] F. Scholze, G. Ulm, "Characterization of a windowless Si(Li) detector in the photon energy range 0.1-5 keV", *Nuclear Instruments and Methods in Physics Research* , A 339 (1994), pp. 49-54

[2] P. Lechner, L. Struder, "Ionization statistics in silicon X-ray detectors - new experimental results", *Nuclear Instruments and Methods in Physics Research* A 354, (1995), p.464

[3] B. Burke, J. Gregory, M.Bautz, G. Prigozhin, S. Kissel, B. Kosicki, A. Loomis, D. Young, "Soft X-ray Imagers for AXAF", *IEEE Transactions on Electron Devices*, v.44, No.10, October 1997, pp. 1633-1642

[4] G. Prigozhin, J. Woo, J. Gregory, A. Loomis, M. Bautz, G. Ricker, S. Kraft, "Quantum efficiency of X-ray CCDs", *Proc. SPIE*, v. 3301, January 1998, pp. 108-115

[5] J. Benedetto, H. Boesch, "The relationship between ^{60}Co and 10 keV X-ray damage in MOS devices", *IEEE Transactions on Nuclear Science*, NS-33, p. 1318, (1986)

[6] R. Hughes, "Charge carrier transport phenomena in amorphous SiO_2: direct measurement of the drift mobility and lifetime", *Phys. Rev. Letters*, 38, (1973), p. 1333

[7] C. Dozier, D. Brown, "Effect of photon energy on the response of MOS devices", *IEEE Transactions on Nuclear Science*, NS-28, (1981), p. 4142

[8] J. Janesick, T. Elliott, S. Collins, T. Daud, C. Campbell, A. Dingizian, G. Garmire, "CCD advances for X-ray scientific measurements in 1985", *X-ray Instrumentation in Astronomy*, Proc. SPIE, v.597, pp. 365-380, (1986)